*J. Fluid Mech.* (1979), *vol.* 95, *part* 1, *pp.* 141–157
*Printed in Great Britain*


# Reflexion of water waves by a permeable barrier

By C. MACASKILL

Department of Applied Mathematics, University of Adelaide†

(Received 16 December 1978)

The linearized problem of water-wave reflexion by a thin barrier of arbitrary permeability is considered with the restriction that the flow be two-dimensional. The formulation includes the special case of transmission through one or more gaps in an otherwise impermeable barrier. The general problem is reduced to a set of integral equations using standard techniques. These equations are then solved using a special decomposition of the finite depth source potential which allows accurate solutions to be obtained economically. A representative range of solutions is obtained numerically for both finite and infinite depth problems.

## 1. Introduction

This paper deals with the transmission and reflexion of surface waves incident on an infinitely thin vertical barrier, in water of finite depth. Only the two-dimensional problem is considered. The barrier is assumed to have some known permeability, that may vary with depth. This permeability may be identified as $1/C$, where $C$ is a non-dimensional blockage coefficient dependent only on the geometrical dimensions of the barrier (the blockage coefficient concept is discussed in Tuck (1975) chapter 5).

In other words, we may regard the barrier as being perforated by many small pores, with the pores being small when $C$ is large (i.e. low permeability) and large when $C$ is small (high permeability).

In small-amplitude unsteady flows, such as those we are dealing with here, the Bernoulli equation may be linearized. This implies that the acceleration of the fluid across the porous barrier is proportional to the pressure jump across it, specifically,

$$a_c = -\frac{1}{2\rho C}\Delta p, \tag{1.1}$$

where $\rho$ is the density of the fluid, $a_c$ is the fluid acceleration, $\Delta p$ is the pressure jump and $C$ is the blockage coefficient referred to above. In time-sinusoidal flows with a (suppressed) time-dependence $e^{-i\sigma t}$, we know that $a_c = i\sigma V$, where $V$ is the (local) streaming velocity through the barrier, so that (1.1) becomes

$$V = -\frac{\Delta p}{2\rho i\sigma C}, \tag{1.2}$$

which is of similar form to the well-known Darcy law for flow in porous media (Morse & Ingard 1968, p. 252)

$$V = -k\Delta p, \tag{1.3}$$

† Present address: School of Mechanical Engineering, Cranfield Institute of Technology, Cranfield, Bedford, England.

where $k$ is the Darcy coefficient. This quantity is usually determined experimentally and determines the dissipation due to viscous effects. $C$ will be real in an inviscid fluid, so that inclusion of this quantity measures local inertial effects at the barrier. However, if we use the results of Macaskill & Tuck (1978) where both real and imaginary parts for $C$ are obtained for a porous screen, we see that viscous effects may also be included. This means that we have available a quantity akin to a Darcy constant which may be determined theoretically for any viscosity, frequency or ratio of pore size to pore separation. In water wave problems, viscous dissipation is generally of minor importance, but the same is not true for the inertial impedance of the barrier. The method presented in this paper allows the comparison of the efficiency of, say, a loosely packed submerged breakwater with a completely solid one. The main drawback with the method is that thickness effects cannot be modelled, although it could possibly be modified to allow this.

Using a variable permeability also allows the determination of results for solid obstacles with one or more large gaps. One example of such a problem is that treated by Ursell (1947). This problem was that of reflexion of surface waves, in infinite water depth, by a single surface-piercing barrier reaching partway to the bottom. This corresponds to our general variable permeability formulation with $C = \infty$ on the barrier and $C = 0$ everywhere else. In a similar fashion the barrier reaching partway to the surface, treated by Dean (1945), may also be considered. In finite depth, these two problems have been solved (numerically) by Mei & Black (1969). Again, the method described here may be used for verifying and extending the results.

Problems of flow through one or more gaps have been treated by several authors. All previous work, with one exception, has dealt with infinite water depth. The exception is the solution for flow through a single small gap, in finite depth, due to Packham & Williams (1972). Tuck (1975) gives a slightly different but equivalent formulation for this problem, and obtains the same results.

In infinite water depth, reflexion by a barrier with any number of gaps has been treated by both Lewin (1963) and Mei (1966). The solutions obtained are extremely complicated, however, and in both cases no numerical results are presented. For a single gap, both Guiney (1972) and Porter (1972) have obtained solutions and they both present comprehensive results, but a large amount of numerical integration is involved. More recently, Porter (1974) has presented a simpler method than those of Lewin (1963) and Mei (1966) for the general problem of an arbitrary number of gaps. Again, though, no numerical results are presented.

All the above problems are included in the present formulation. In presenting our results for problems with more than one gap, however, only the problem with two gaps of equal size, in water of infinite depth, is used. This is merely to reduce the number of parameters in the problem (e.g. gap width/gap separation, gap width/mean depth of submersion of two gaps etc.) so that some valid conclusions may be drawn. The method is easily applicable to more than two gaps (at the expense of a small increase in computing time) but to give a proper coverage of results for such problems would be extremely laborious and would convey very little extra information.

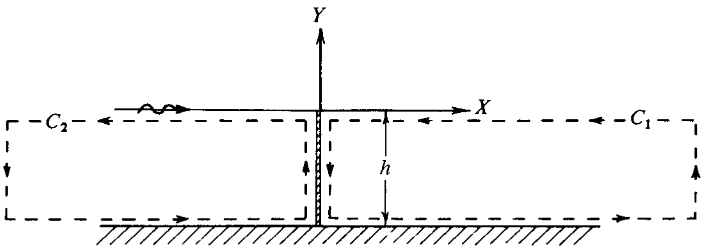


FIGURE 1. Schematic diagram of the permeable barrier.

## 2. Mathematical formulation

A similar formulation to the following was outlined briefly by Tuck (1975) for the thin barrier problem in water of infinite depth. In the present work it is assumed that the depth is finite, but is everywhere constant. In the limit as the depth approaches infinity, it is shown that Tuck's result is regained.

Cartesian co-ordinates $x$ and $y$ are used (see figure 1). The fluid is assumed non-viscous and the flow irrotational, so that a velocity potential $\Phi(x, y, t)$ exists which satisfies Laplace's equation,

$$\nabla^2 \Phi = 0, \tag{2.1}$$

everywhere in the fluid.

Sinusoidal time-dependence is assumed so that a complex-valued potential function $\phi(x, y)$ may be introduced, where

$$\Phi(x, y, t) = \operatorname{Re}[\phi(x, y)\, e^{-i\sigma t}] \tag{2.2}$$

and $\sigma$ is the wave frequency.

Since the waves are assumed to be of small amplitude, the linearized free surface condition may be used, that is

$$\partial\phi/\partial y - \nu\phi = 0, \quad y = 0, \tag{2.3}$$

where $\nu = \sigma^2/g$ and $g$ is the acceleration due to gravity. There must also be no normal fluid velocity on the bottom $y = -h$, so that

$$\partial\phi/\partial y = 0, \quad -\infty < x < \infty. \tag{2.4}$$

Plane progressive waves of unit amplitude are incident from $x = -\infty$, so that $\phi$ takes the form

$$\phi \to (e^{iKx} + Re^{-iKx}) \frac{\cosh K(y+h)}{\cosh Kh} \tag{2.5}$$

and

$$\phi \to \tau\, e^{iKx} \frac{\cosh K(y+h)}{\cosh Kh} \tag{2.6}$$

where $R$ and $\tau$ are the complex-valued reflexion and transmission coefficients. $K$ is the characteristic wavenumber for waves of frequency $\sigma$ in water of depth $h$, given by

$$\nu = K \tanh Kh. \tag{2.7}$$

It is also necessary to define a Green's function $G(x, y; \xi, \eta)$ satisfying the boundary conditions (2.3) and (2.4), and the equation

$$\nabla^2 G = \delta(x-\xi)\,\delta(y-\eta). \tag{2.8}$$

$G$ must also satisfy suitable radiation conditions at $x = \pm\infty$; specifically, it should behave like an outgoing wave. Several forms for $G$ may be found in Wehausen & Laitone (1960), p. 483 – we postpone discussion of the most suitable choice.

If Green's theorem is now applied to the circuit $C_1$, on the right-hand side of the barrier in figure 1, then

$$\phi(\xi,\eta) = \oint_{C_1} \phi(x,y)\frac{\partial G}{\partial n}(x,y;\xi,\eta) - G(x,y;\xi,\eta)\frac{\partial \phi}{\partial n}(x,y)\,dl. \tag{2.9}$$

The only contribution to the integral in (2.9) comes from the arc $-h < y < 0, x = 0_+$. There is no contribution from the free surface or the bottom, since both $\phi$ and $G$ satisfy (2.3) and (2.4). At $x = \infty$, since both $\phi$ and $G$ behave like outgoing waves, there is again no contribution to the integral. Thus (2.9) becomes

$$\phi(\xi,\eta) = \int_{-h}^{0} \frac{\partial \phi}{\partial x}(0_+,y)\,G(0_+,y;\xi,\eta) - \phi(0_+,y)\frac{\partial G}{\partial x}(0_+,y;\xi,\eta)\,dy. \tag{2.10}$$

If we apply Green's theorem over the circuit $C_2$ we obtain in a similar manner

$$\phi(\xi,\eta) = \phi_0(\xi,\eta) - \int_{-h}^{0} \frac{\partial \phi}{\partial x}(0_-,y)\,G(0_-,y;\xi,\eta)\,dy + \int_{-h}^{0} \phi(0_-,y)\frac{\partial G}{\partial x}(0_-,y;\xi,\eta)\,dy. \tag{2.11}$$

In this case there is a contribution from the part of the circuit at $x = -\infty$ since $\phi$ has an incoming component. Specifically, this contribution is

$$\phi_0 = \frac{\cosh K(\eta+h)\,e^{iK\xi}}{\cosh Kh}. \tag{2.12}$$

In equations (2.10) and (2.11), we have available solutions for $x \geqslant 0$ and $x \leqslant 0$ separately. To complete this formulation we need to match the two equations across $x = 0$. Since $\partial G/\partial x$ behaves like a delta function as $\xi \to x$, (2.10) becomes, with $\xi \to 0_+$,

$$\phi(0_+,\eta) = 2\int_{-h}^{0} \frac{\partial \phi}{\partial x}(0_+,y)\,G(0_+,y;0_+,\eta)\,dy, \tag{2.13}$$

while (2.11) reduces to

$$\tfrac{1}{2}\phi(0_-,\eta) = \phi_0(0_-,\eta) - \int_{-h}^{0} \frac{\partial \phi}{\partial x}(0_-,y)\,G(0_-,y;0_-,\eta)\,dy \tag{2.14}$$

as $\xi \to 0$. To obtain a final integral equation from (2.12) and (2.13) requires some form of matching condition across $x = 0$, $-h < y < 0$. Problems where the barrier is made up of impermeable material perforated by large totally permeable gaps are easily treated and we therefore consider these first. We refer to figure 2.

Across all open sections $y \in L_m$, $m = 1, \ldots, M$, there is no flow restriction across $x = 0$, so that

$$\frac{\partial \phi}{\partial x}(0_-,y) = \frac{\partial \phi}{\partial x}(0_+,y) = \frac{\partial \phi}{\partial x}(0,y) \tag{2.15}$$

and

$$\phi(0_-,y) = \phi(0_+,y) = \phi(0,y) \quad y \in L_m, \quad x = 0. \tag{2.16}$$

For all other points on $x = 0$, there is no flow at all, since the barrier is totally impermeable. This means that the normal velocity across the barrier must be zero at

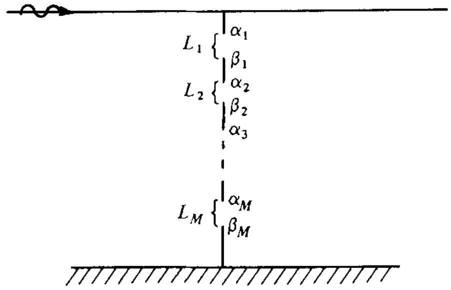


FIGURE 2. Schematic diagram of a many-gap barrier.

these points, although there may be a discontinuity in the potential function. This condition we write as

$$\frac{\partial\phi}{\partial x}(0_+,y) = \frac{\partial\phi}{\partial x}(0_-,y) = 0, \quad y \notin L_m, \quad x = 0. \tag{2.17}$$

On using these conditions, and observing that the Green's function $G$ is continuous across $x = 0$, we may reduce (2.13) and (2.14) to the single integral equation

$$\sum_{m=1}^{M} 2\int_{L_m} \frac{\partial\phi}{\partial x}(0,y)\, G(0,y,0,\eta)\, dy = \frac{\cosh K(\eta+h)}{\cosh Kh}. \tag{2.18}$$

This equation may be discretized and solved numerically for any barrier configuration that may be described as a series of disconnected arcs $L_m$. The problems treated by Porter (1972), Dean (1945) and Ursell (1947), for example, may all be treated in this way.

The problem becomes more involved if the permeability is no longer either zero or infinite as in the above examples. There is now the possibility of an effective potential jump across $x = 0$ at points where the velocity is non-zero. Subtracting (2.14) from (2.13) gives

$$\begin{aligned}\Delta\phi &= \phi(0_+,\eta) - \phi(0_-,\eta)\\ &= 2\int_{-h}^{0} G(0,y,0,\eta)\left[\frac{\partial\phi}{\partial x}(0_+,y) + \frac{\partial\phi}{\partial x}(0_-,y)\right] dy - 2\phi_0(0,\eta).\end{aligned} \tag{2.19}$$

In this equation we have implicitly assumed the continuity of $G$ and $\phi_0$ across $x = 0$. It now is necessary to use the concept of a blockage coefficient $C$, as defined in the introduction. For non-zero finite permeability, the barrier at $x = 0$ may be considered to be perforated by some (assume given) array of small pores. The local flow at any point on $x = 0$ may then be regarded as unsteady streaming flow through a screen. At each point $y$ on $x = 0$ the screen will have some local permeability or blockage coefficient $C(y)$. At a distance from the barrier that is large compared with the average pore size, but still is small when compared with all other dimensions in the problem, the flow will tend to

$$\phi(x,y) \rightarrow U(y)\,x + U(y)\,C(y)\,\mathrm{sgn}\,x, \tag{2.20}$$

where $U(y)$ is the streaming velocity appropriate for any point $(0,y)$. Since the distance from the barrier is still small, in terms of the outer flow, $U$ may be recognized as

$$U = \phi_x(0_+,y) = \phi_x(0_-,y) = \phi_x(0,y). \tag{2.21}$$

This means that there is no jump in velocity across the barrier as far as the outer flow pattern is concerned. By (2.20), however, there is a jump in the velocity potential, given by

$$\Delta\phi = 2\phi_x(0,y)\,C(y) \tag{2.22}$$

so that (2.19) becomes

$$\phi_x(0,\eta)\,C(\eta)+\phi_0(0,\eta) = 2\int_{-h}^{0} G(0,y;0,\eta)\frac{\partial\phi}{\partial x}(0,y)\,dy. \tag{2.23}$$

It must be noted that for validity of the above reasoning, the length scale for variation in $C(y)$ must be much larger than the length scale for the pores in the breakwater. It should be noted, too, that viscous dissipative effects may be included by introducing an imaginary component in the blockage coefficient.

Since $C(y)$ is assumed known (determined theoretically perhaps as in Macaskill & Tuck (1977) or obtained experimentally), equation (2.23) constitutes an integral equation of the second kind in the normal velocity across $x = 0$.

Equation (2.18) may also be regarded as a special case of (2.23). For

$$y \in L_m, \quad m = 1, \ldots, M,$$

the blockage coefficient is zero. For all other points the normal velocity is zero. Using these two facts, we may immediately recover (2.18) from (2.23).

Finally, Tuck's (1975) infinite depth formulation may be recovered by allowing $h \to \infty$ in (2.23) so that

$$C(\eta)\,\phi_x(0,\eta)+e^{\kappa\eta} = 2\int_{-\infty}^{0} G_\infty(0,y;0,\eta)\frac{\partial\phi}{\partial x}(0,y)dy, \tag{2.24}$$

where $G_\infty$ is the limiting form of $G$ as $h \to \infty$. This limiting form is well known, and is indeed a great deal simpler than $G$ for finite depth. Thus, for problems where the depth is very large, the infinite depth Green's function will be used (see Wehausen and Laitone, 1960).

## 3. Numerical analysis

There are now two forms of the integral equation that may be used, depending on the nature of the breakwater, namely (2.18) and (2.23).

First we consider the numerical solution of equation (2.23). We use a simple collocation method first proposed by Tuck (1969) and since then used with success by others.

In (2.23) we assume that $\phi_x$ is slowly varying at $x = 0$. We divide the arc $x = 0$, $0 \geqslant y \geqslant -h$ into $N$ segments $(y_j, y_{j+1})$ with $y_j > y > y_{j+1}$, $j = 1, \ldots, N$. Then, the approximation $\phi_x(0,y) = \phi_{xj} =$ constant is made. We must now make a choice of meshpoints. So long as the blockage coefficient $C(y)$ is slowly varying, the obvious choice is a uniform distribution of points. For the special case described by equation (2.18), where we have introduced sharp corners at the end of each arc $L_m$, we may make a better choice. We know that in the near vicinity of these corners the velocity potential has a square-root singularity, so on $L_m = (\alpha_m, \beta_m)$, for example, we take

$$y_{j,m} = \alpha_m + \left[\sin\frac{\pi}{2}\left(\frac{k}{N}\right)\right](\beta_m-\alpha_m), \quad j = 1,2,\ldots,N+1 \quad \text{with} \quad k = 2(j-1)-N. \tag{3.1}$$

These Chebychev points automatically account for the expected square root singularity in the velocity at these corners. It should be noted that a separate set of meshpoints $y_{j,m}$, $j = 1, \ldots, N$, is required for each arc $L_m$.

We satisfy the integral equation at the $N$ points

$$\eta_i = \left(\frac{y_i + y_{i+1}}{2}\right), \quad i = 1, \ldots, N, \tag{3.2}$$

for problems with slowly varying $C(y)$. For problems involving one or more large gaps, as described by equation (2.18), we choose

$$\eta_{i,m} = \alpha_m + \left[\sin\frac{\pi}{2}\left(\frac{k}{N}\right)\right](\beta_m - \alpha_m), \quad i = 1, \ldots, N \quad \text{with} \quad k = 2i - 1 - N, \tag{3.3}$$

which is consistent with the choice of meshpoints $y_j$ in equation (3.1).

With these assumptions, (2.23) may be written in discrete form as

$$\phi_{xi} C_i + \phi_{0i} = 2 \sum_{j=1}^{N} \phi_{xj} \int_{y_j}^{y_{j+1}} G(0, y_j; 0, \eta_i)\, dy, \quad i = 1, \ldots, N, \tag{3.4}$$

where $\phi_{0i}$ represents the obvious discretization $\phi_0(0, \eta_i)$. In a similar way we may write (2.18) as

$$\phi_{0i,m} = 2 \sum_{j=1}^{N} \phi_{xj,m} \int_{y_{j,m}}^{y_{j+1,m}} G(0, y_{j,m}; 0, \eta_{i,m})\, dy \tag{3.5}$$

for $i = 1, \ldots, N$; $m = 1, \ldots, M$.

Thus (3.4) becomes

$$A^* \mathbf{\Phi} = \mathbf{\Phi}_0, \tag{3.6}$$

where

$$A^* = 2[A_{ij}] - [C_i \delta_{ij}], \tag{3.7}$$

and

$$A_{ij} = \int_{y_j}^{y_{j+1}} G(0, y_j; 0, \eta_i)\, dy, \tag{3.8}$$

$$\mathbf{\Phi} = (\phi_{x1}, \ldots, \phi_{xN})^t, \tag{3.9}$$

and

$$\mathbf{\Phi}_0 = (\phi_{01}, \ldots, \phi_{0N})^t. \tag{3.10}$$

Equation (3.5) may be represented in similar fashion. It should be noted in (3.5) that increasing the number of gaps generally increases the amount of computing time required to solve the problem, since introducing extra singularities (by way of more corners) will increase the number of points required to obtain satisfactory accuracy.

Once we have the problem in the form (3.6), with $(A_{ij})$ known, we can find the normal velocity through the gap by inverting the matrix equation. Once the normal velocity has been obtained, the transmission and reflexion coefficients may be obtained from the original integral equations, using the limiting form as $\xi \to \pm\infty$.

The only remaining problem is the actual evaluation of the elements $A_{ij}$. We consider the general problem of evaluating the finite depth Green's function in the next section. In the special case when the depth is infinite, or very large, it is more desirable to use the infinite-depth Green's function. For these problems we truncate the range of integration from the interval $(0, -\infty)$ to say $(0, -h^*)$. Our choice of mesh points is now the same as for finite depth problems with $h^*$ replacing $h$. This means that we are actually assuming a solid barrier for $y < -h^*$. In practice this should not affect the transmission, so long as $h^*$ is chosen large enough, as there is exponential decay in the wave motion of the form $e^{Ky}$. The only other change we make is in the evaluation of the elements $A_{ij}$, which now become

$$A_{ij} = \int_{y_j}^{y_{j+1}} G_\infty(0, y_j; 0, \eta_i)\, dy, \tag{3.11}$$

where $G_\infty$ is the infinite depth Green's function referred to in § 2. A convenient form of this function is

$$G_\infty = \frac{1}{2\pi}(\log|y-\eta| - \log|y+\eta|) - \frac{1}{\pi} ⨍_0^\infty \frac{e^{p(y+\eta)}}{p-K}\, dp - i\, e^{K(y+\eta)}. \tag{3.12}$$

We may immediately write $A_{ij}$ as

$$A_{ij} = \left[\frac{y-\eta}{2\pi}\log|y-\eta| - \frac{(y+\eta)}{2\pi}\log|y+\eta| - \frac{i\,e^{K(y+\eta)}}{K}\right]_{y_j}^{y_{j+1}} - \frac{1}{\pi}\int_{y_j}^{y_{j+1}} ⨍_0^\infty \frac{e^{p(y+\eta)}}{p-K}\, dp\, dy. \tag{3.13}$$

On interchanging the order of integration in the integral in (3.13) we may finally determine $A_{ij}$ as

$$A_{ij} = \left[\frac{y-\eta}{2\pi}\log|y-\eta| - \frac{y+\eta}{2\pi}\log|y+\eta| - \frac{i\,e^{K(y+\eta)}}{K} - \frac{1}{K\pi}\log|y+\eta| + \frac{1}{K\pi}e^{K(y+\eta)}\,\overline{\mathrm{Ei}}(-K(y+\eta))\right]_{y_j}^{y_{j+1}}. \tag{3.14}$$

Here $\overline{\mathrm{Ei}}(x)$ is the exponential integral (see Abramowitz & Stegun 1964). This function may be quickly and easily computed for all values of its argument with the use of polynomial approximations.

## 4. Evaluation of the Green's function

In determining the elements $A_{ij}$ we require an efficient method for evaluating the indefinite integral of the finite depth Green's function. This section details such a method. An alternative approach would be to determine a good way of finding the function itself, rather than its integral, and then to use numerical integration to obtain the matrix elements $A_{ij}$. Although the present problem has been set up so as to avoid this numerical integration, in many other problems this cannot be done. Thus an efficient method for evaluating the Green's function itself is also of interest. For example, Sheridan (1975) describes a straightforward method for determining the Green's function. It is thought that the method described here is a distinct improvement, especially in the present case where we are interested in $x = \xi = 0$.

Two forms of the Green's function are available. One is an integral representation

$$G(x,y;\xi,\eta;h) = \frac{1}{2\pi}\left[\log\left(\frac{[(x-\xi)^2+(y-\eta)^2]^{\frac{1}{2}}}{h}\right) + \log\left(\frac{[(x-\xi)^2+(y+\eta+2h)^2]^{\frac{1}{2}}}{h}\right)\right] - \frac{1}{\pi}\int_0^\infty \left(e^{-kh}\, G_B \cosh k(h+y)\cos k(x-\xi) - \frac{e^{-kh}}{k}\right) dk - iG_A \cos K(x-\xi)\cosh K(y+h), \tag{4.1}$$

where

$$G_A = \frac{\nu+K}{K}\,\frac{e^{-Kh}\sinh kH \cosh K(h+\eta)}{\nu h + \sinh^2 Kh} \tag{4.2}$$

and
$$G_B = \frac{\nu+k}{k}\,\frac{\cosh k(h+\eta)}{k\sinh kh-\nu\cosh kh}. \tag{4.3}$$

Alternatively, the function can be expressed in terms of the series expansion

$$G(x,y;\xi,\eta;h) = -\sum_{n=1}^{\infty} P_n \cos m_n(y+h)\exp[-m_n|x-\xi|] \\ -iG_A \exp[+iK|x-\xi|]\cosh K(y+h), \tag{4.4}$$

where $G_A$ is given by equation (4.2) and

$$P_n = \frac{1}{m_n}\,\frac{m_n^2+\nu^2}{hm_n^2+h\nu^2-\nu}\cos m_n(\eta+h). \tag{4.5}$$

The $m_n$'s, $n = 1,\ldots,\infty$, are the real roots of the equation

$$-m_n \tan m_n h = \nu. \tag{4.6}$$

For a derivation of the above forms and other alternative formulations, reference should be made to either Wehausen and Laitone (1960) or Thorne (1953).

In the special case $x = \xi = 0$ equation (4.4) takes on a very simple form. It is not, however, particularly suitable for numerical computations, as it is extremely slowly convergent [this is due to the presence of the logarithmic singularities shown explicitly in equation (4.1)]. The integral form, by contrast, does not pose this problem but we do have to deal with an oscillatory integral over an infinite range of integration (the singularity poses few problems). This integral can be evaluated numerically with some success but it is difficult to obtain high accuracy and such methods are not very efficient.

We find that a more economical procedure is to rearrange equation (4.4) so that the logarithmic singularity appears explicitly. Convergence is then rapidly obtained without the attendant complications involved when using the integral representation.

We rewrite (4.4) for convenience as (with $x = \xi = 0$)

$$G(0,y;0,\eta;h) = -\sum_{m=1}^{\infty} Q_n(0,y;0,\eta;h) - iG_A\cosh K(y+h), \tag{4.7}$$

where
$$Q_n = P_n \cos m_n(y+h). \tag{4.8}$$

For moderate values of the non-dimensional parameter $\nu h$, as $n\to\infty$ it can be shown that

$$m_n \to \frac{n\pi}{h} + O(n^{-1}), \tag{4.9}$$

so that, as $n \to \infty$,

$$Q_n \to \frac{1}{n\pi}\cos\frac{\pi n}{h}(y+h)\cos\frac{\pi n}{h}(\eta+h) = Q_n^*. \tag{4.10}$$

We now consider the behaviour of

$$R(0,y;0,\eta;h) = \sum_{n=1}^{\infty}\frac{1}{n\pi}\cos\frac{\pi n}{h}(y+h)\cos\frac{\pi n}{h}(\eta+h). \tag{4.11}$$

This series is only slowly convergent. Because of this the expansion (4.4) for $G$ is also slowly convergent. It is possible, however, to evaluate $R(0, y; 0, \eta; h)$ exactly. We write

$$R(0,y;0,\eta;h) = \frac{1}{2}\sum_{n=1}^{\infty}\frac{1}{n\pi}\cos\frac{\pi n}{h}(y+\eta+2h) + \frac{1}{2}\sum_{n=1}^{\infty}\frac{1}{n\pi}\cos\frac{\pi n}{h}(y-\eta) \quad (4.12)$$

$$= R_1(0,y;0,\eta;h)+R_2(0,y;0,\eta;h). \quad (4.13)$$

We consider only the second series $R_2$ (the first is almost the same). We put

$$Y = \pi/h(y-\eta). \quad (4.14)$$

Then $R_2$ is given by

$$R_2(0,y;0,\eta;h) = \tfrac{1}{2}\pi\sum_{n=1}^{\infty}\frac{\cos ny}{n}. \quad (4.15)$$

This series may be summed immediately (see Abramowitz & Stegun, 1964), so that

$$R_2(0,y;0,\eta;h) = -\frac{1}{2\pi}\log 2\sin\frac{\pi}{2h}|y-n|. \quad (4.16)$$

A similar expression may be derived for $R_1$. Once an exact expression for $R$ has been determined we are immediately in a position to reorganize the Green's function (4.7) so that it may be efficiently computed. We write

$$G(0,y;0,\eta;h) = -iG_A\cosh K(y+h) - \sum_{n=1}^{\infty}(Q_n - Q_n^*) - R(0,y;0,\eta;h). \quad (4.17)$$

Since as $n$ becomes larger $Q_n \to Q_n^*$ the summation in (4.17) is highly convergent. Because of this, very few terms will give a good approximation. It should be remembered, however, that this method does not overcome the problem of slow convergence for large values of the parameter $\nu h$ (i.e. for very short waves), since then the approximation (4.9) does not hold until $n$ becomes large. This sort of problem is, of course, also present when the standard representations (4.1) and (4.7) are used. This is a separate problem in evaluating these Green's functions, and as yet no simple method has been found to overcome it.

It should not be noted that the above procedure can also be applied when $x$ and/or $\xi$ are non-zero. Reference should be made to Macaskill (1977) for details.

At this stage, some comparison of (4.17) and (4.7) is in order. In table 1 we show the results obtained with the two methods for various numbers of terms in the infinite series. As can be seen, (4.17) is markedly superior. The table also shows that the efficiency of either method degrades as the parameter $\nu h$ increases.

Using (4.4), we may now determine the elements $A_{ij}$.

We require

$$I = \int_{y_j}^{y_{j+1}} G(0,y;0,\eta;h)\,dy, \quad (4.18)$$

where $\eta$ may take any value. If we carry out a direct integration on equation (4.4) substituting for the values of $R$, $Q_n^*$ and $Q_n$ using (4.16), (4.10) and (4.8) respectively, we find

$$I = \left[-iG_A/K\sinh K(y+h) + \sum_{n=1}^{\infty} Ln\right]_{y_j}^{y_{j+1}} - \frac{1}{2\pi}\int_{y_j}^{y_{j+1}}\log 4\sin\frac{\pi(y-\eta)}{2h}\sin\pi\frac{(y+\eta+2h)}{2h}\,dy, \quad (4.19)$$

| $Kh$ | $Ky$ | $K\eta$ | No. of terms | New method Re $G$ | Series Re $G$ |
|---|---|---|---|---|---|
| 1 | −0·35 | −0·4 | 10 | −0·1851856 | −0·2568542 |
| 1 | −0·35 | −0·4 | 100 | −0·1850087 | −0·1840531 |
| 1 | −0·35 | −0·4 | 1000 | −0·1850087 | −0·1851612 |
| 1 | −0·35 | −0·4 | 10000 | −0·1850087 | −0·1850253 |
| 1 | −0·35 | −0·95 | 10 | 0·1496019 | 0·1497054 |
| 1 | −0·35 | −0·95 | 100 | 0·1495876 | 0·1480071 |
| 1 | −0·35 | −0·95 | 1000 | 0·1495876 | 0·1494285 |
| 1 | −0·35 | −0·95 | 10000 | 0·1495876 | 0·1495717 |
| 1 | −0·96 | −0·95 | 10 | −0·8230905 | −0·7548512 |
| 1 | −0·96 | −0·95 | 100 | −0·8230853 | −0·8334187 |
| 1 | −0·96 | −0·95 | 1000 | −0·8230851 | −0·8230820 |
| 1 | −0·96 | −0·95 | 10000 | −0·8230851 | −0·8230994 |
| 1 | −0·05 | −0·06 | 10 | −0·7050828 | −0·6056878 |
| 1 | −0·05 | −0·06 | 100 | −0·7068106 | −0·7170789 |
| 1 | −0·05 | −0·06 | 1000 | −0·7068104 | −0·7068079 |
| 1 | −0·05 | −0·06 | 10000 | −0·7068104 | −0·7068247 |
| 10 | −5 | −6 | 10 | −0·3892591 | −0·3856073 |
| 10 | −5 | −6 | 100 | −0·3935326 | −0·3949584 |
| 10 | −5 | −6 | 1000 | −0·3935325 | −0·3936899 |

TABLE 1. The improvement in calculating Green's function for $x = 0$ over numerical summation of the standard series.

where $$Ln = P_n/m_n \sin m_n(y+h) - \frac{h}{n^2\pi^2}\sin\frac{n\pi}{h}(y+h)\cos\frac{n\pi}{h}(\eta+h). \tag{4.20}$$

These calculations were performed on a CDC 6400 computer. It was found that the reflexion coefficient could be determined to three decimal place accuracy with a twenty-point mesh for values of non-dimensional frequency $\nu h$ up to about five. With this number of points approximately three seconds was required to set up the matrix and two to invert it. As the number of mesh points was increased (e.g. to deal with many gap problems or to look at high frequency limits) it was found that a higher percentage of time was spent on the matrix inversion. Thus a forty-point calculation took about twenty-five seconds, only half of this time being used to set up the matrix. For problems of infinite depth, set-up time was generally less than matrix inversion time. For a forty-point mesh, core required was approximately 25 kilowords.

## 5. Results

We consider first problems of the type described by equation (2.18). Any results given for infinite depth were computed using the infinite depth Green's function, as given in (3.12), in preference to using the finite depth Green's function with a large depth parameter.

The first set of curves is for flow past a surface-piercing barrier of height $l$ in water depth $h$. This is the problem first treated by Ursell (1947), for water of infinite depth. In figure 3 the transmission coefficient is plotted against $\nu l$. The present work agrees

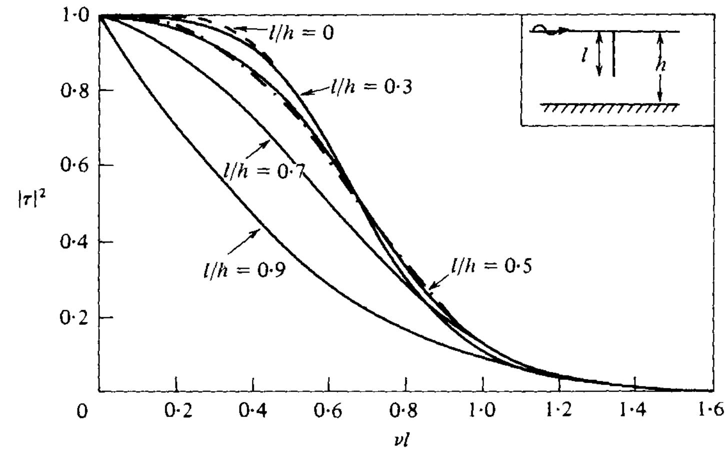


FIGURE 3. Transmission coefficient for a surface-piercing barrier. ——, Ursell (1947), $l/h = 0$; —·—, Mei & Black (1969), $l/h = 0{\cdot}5$.

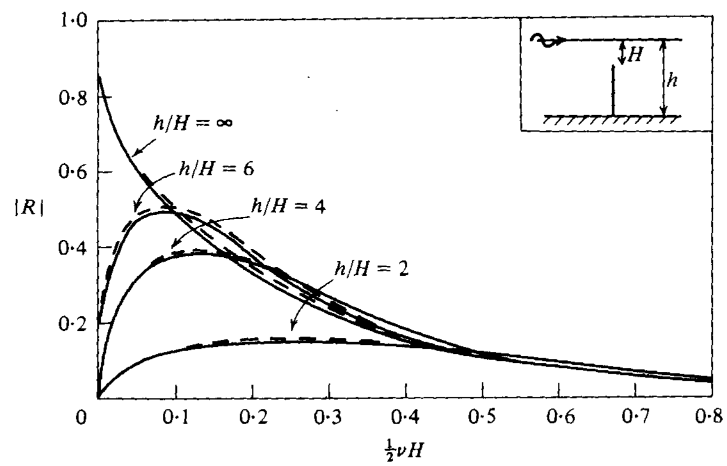


FIGURE 4. Reflexion coefficient for a single barrier reaching partway to the surface in water of finite depth. ----, Mei & Black (1969).

very well with Ursell's results – the two results are indistinguishable on the scale shown. When the depth is finite, certain interesting trends become apparent.

As $l/h$ becomes larger, the opening closes off more and more – this is indicated by a general reduction in the transmission coefficient. For values of $l/h$ in the range $0{\cdot}5$–$0{\cdot}7$ it can be seen, by contrast, that the transmission coefficient is actually higher than Ursell's results for waves of moderate frequency. At high frequency, however, all curves collapse on to the infinite depth result.

For $l/h = 0{\cdot}5$ a result due to Mei & Black (1969) is shown. At low frequency, there is some small disparity with the present work. At high frequency, however, the two curves both collapse on to the infinite-depth result.

In fact, although it is not shown in figure 3, the result of Mei & Black for $l/h = 0$ shows good agreement with both the present results and with the theory of Ursell.

In figure 4 results are displayed for the situation where there is a single vertical barrier extending from the bottom partway to the surface. This is in a sense complementary to the surface-piercing barrier problem. Indeed, the analytic solution by Dean (1945), for the case of infinite depth, appeared only a few years before Ursell's paper. For convenience, we show the magnitude of the reflexion coefficient rather than that of the transmission coefficient. The present work again shows excellent agreement with Dean's result and the answers obtained are essentially the same. For finite depth, extensive results have been given by Mei & Black (1969). As can be seen, the agreement between the two theories is very good over the whole range of frequency for all values of the parameter $h/H$. It should be noted that the variational method used by Mei & Black (1969) becomes less accurate as $h/H$ increases. This is because the method involves approximating an infinite series by taking the first few terms. The fact that the disparities between the two methods become more marked as $h/H$ increases is probably a consequence of this, since the present method gives equally good accuracy for all $h/H$, at least at low frequency. That the variational method overestimates the reflexion coefficient seems to be borne out by the comparison with Dean (1945) for infinite depth. All in all, though, agreement is very good.

We now turn to the problem of transmission through a single gap in a vertical wall. For infinite depth, this problem has been solved exactly by Porter (1972) and Guiney (1972), while an earlier theory by Tuck (1971) solves the problem when the gap is small. In this case, it is convenient to define a parameter $\mu = 2a/H$ where $2a$ is the gap width and $H$ the mean depth of the gap. It was found that over the full frequency range, at any value of $\mu$, excellent agreement was obtained with the exact theory of Guiney. The results of Porter appear to be the same. Since both exact methods require a large amount of numerical integration to obtain final answers, it is possible that the present method is preferable for these problems, since good accuracy can be obtained rapidly and easily, and the present method is more flexible.

For flow through a single gap in finite depth, there are no published results for arbitrary $\mu$. However, for small gaps, both Tuck (1975) and Packham & Williams (1972) have obtained solutions that agree very well. Comparison of Tuck's result with the present work, at $\mu = 0{\cdot}15$, showed almost exact agreement, even at high frequency. This indicates that the small-gap theory is very good for $\mu$ of this order. For completeness, results obtained by the present method are displayed in figure 5 for $\mu = 0{\cdot}15$. As has been said, however, the results are for all practical purposes identical with those published elsewhere. Unfortunately, no small-gap results are available for larger $\mu$. It is quite likely that the small-gap approach would be successful for quite large $\mu$, especially at low frequency. (Surprisingly good agreement has been demonstrated for infinite depth (see, e.g., Tuck, 1975).

In figures 6 and 7 the magnitude of the transmission coefficient is plotted for various values of $H/h$ with $\mu = 0{\cdot}5$ and $1{\cdot}0$ respectively. As can be seen, no qualitative change from the small gap problem is apparent. In a quantitative sense, transmission increases as the gap becomes bigger, as might be expected.

We now turn to flow problems with more than one gap. For simplicity, only infinite depth results are presented, although the method works just as well for finite depth. Both gaps are assumed to be of width $2a$, with their centres separated by a distance $b$. In figures 8 and 9 the transmission coefficient is plotted for various values of $b/H$, where $H$ is the mean depth of submersion of the *upper* gap. The limiting curve $b/H = 1$ corresponds to the two gaps being side by side, so forming a single gap of width $4a$. Thus the results obtained should be the same as for a single gap with $\mu = \frac{4}{3}$. This in

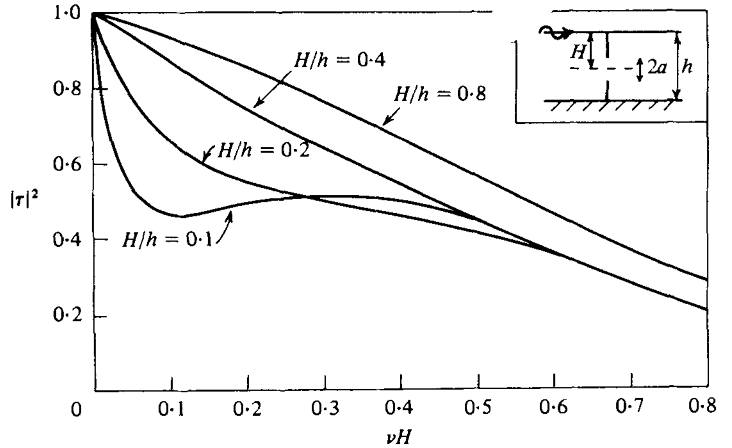


FIGURE 5. Water wave transmission through a single-gap barrier in water of finite depth ($\mu = 2a/H = 0{\cdot}15$).

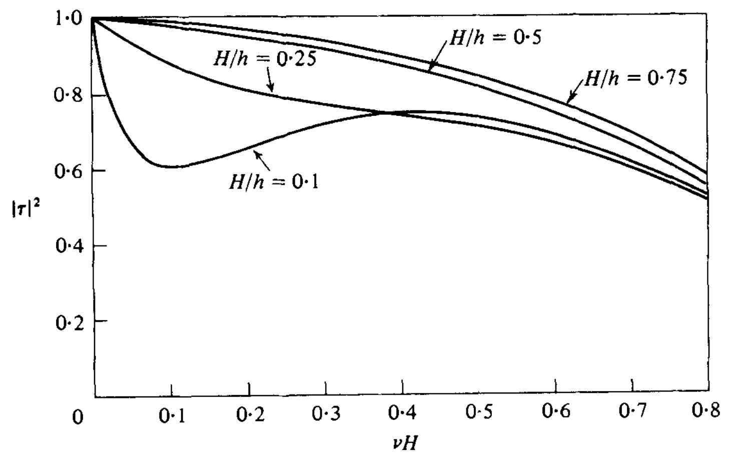


FIGURE 6. Water wave transmission through a single-gap barrier in water of finite depth ($\mu = 2a/H = 0{\cdot}5$). $H$, $a$ and $h$ as defined on figure 5.

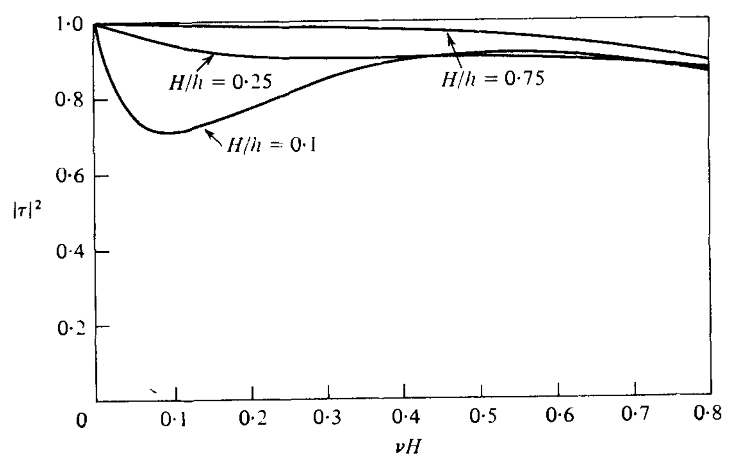


FIGURE 7. Water wave transmission through a single-gap barrier in water of finite depth ($\mu = 2a/H = 1{\cdot}0$). $H$, $a$ and $h$ are defined on figure 5.

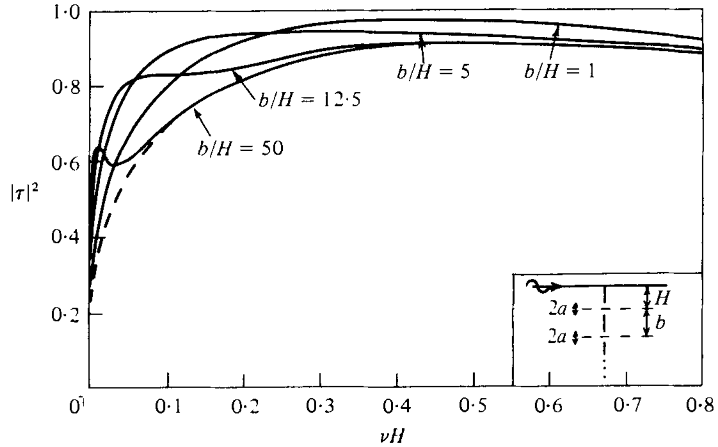


FIGURE 8. Water wave transmission through a two-gap barrier in water of infinite depth ($\mu = 1·0$). ---, single-gap result.

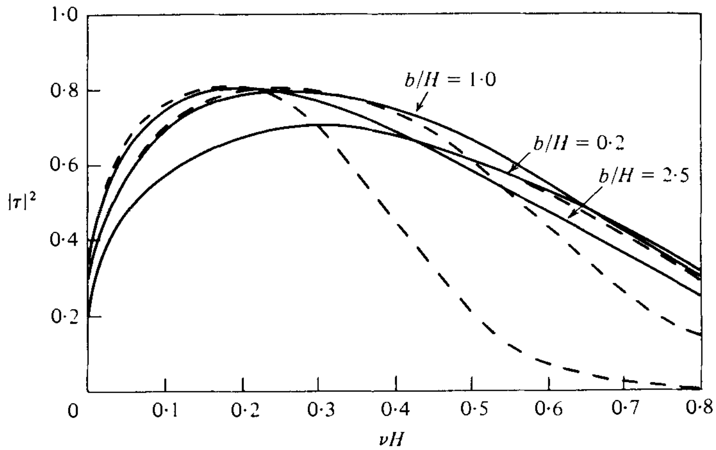


FIGURE 9. Water wave transmission through a two-gap barrier in water of infinite depth ($\mu = 0·2$). ---, the small gap theory of Tuck (1976). $H$, $a$ and $b$ are defined on figure 8.

fact turns out to be the case, with the results agreeing exactly with those obtained for the single-gap problem. We now increase the value of $b/H$. This corresponds to holding the top gap in place while moving the bottom one down. At low frequency, the incoming wave appears to see less impedance than would be the case if there were no interaction effects. Thus the transmission coefficient is larger than for the $b/H = 1$ curve. At higher frequency this is no longer true and in fact the transmission coefficient is smaller than the $b/H = 1$ value. This is probably because short waves are confined to a thin surface layer and so cannot 'feel' the deeply submerged bottom gap. As $b/H$ becomes larger it is interesting to note that a definite peak becomes apparent in the transmission coefficient, at reasonably low frequency. This indicates that some sort of resonance effect is taking place owing to the interaction of the flow with the two gaps. It is possible that in many-gap problems we might obtain a large number of peaks of this form, although this has not been checked.

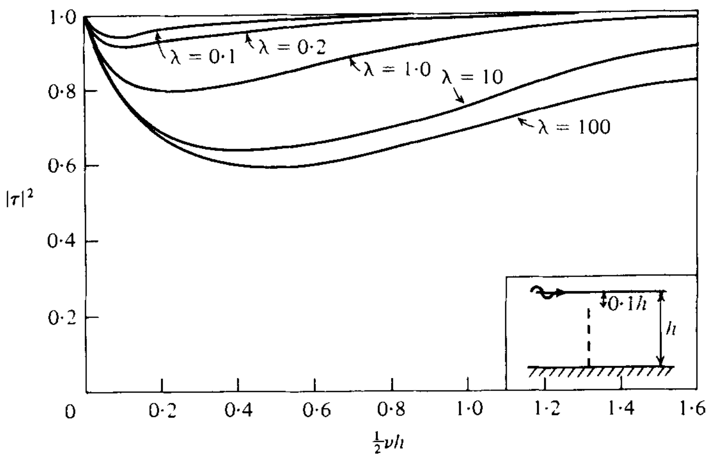


FIGURE 10. Transmission coefficient for a semi-permeable barrier. Large $\lambda$ corresponds to low porosity.

As $b/H$ becomes very large, we expect the transmission coefficient curve to collapse down to that for a single gap of width $2a$, since the waves on the surface are not affected by the deeply submerged lower gap. Indeed this is so and we see that, for values of $\nu H$ greater than 0·1, the $b/H = 50$ curve agrees with that for a single gap with $\mu = 1{\cdot}0$.

For small gaps, Tuck (1975) has postulated that an array of gaps may be regarded in the far field as a single gap, of suitable width, if the gap separation and gap width are small compared to the mean depth of submersion of the array. This theory was tested in figure 9 for two holes of equal width with $\mu = 0{\cdot}2$. Tuck (1975) predicts that the effective gap width of the two gaps is $(b^2-a^2)^{\frac{1}{2}}$. Using this result in his single-gap theory for small gaps we obtain the dotted line solution shown in figure 9. As can be seen, for small-gap separation, the agreement is very good, even at reasonably high frequency.

For larger gap separation, however, the assumptions behind Tuck's (1975) theory break down and the agreement with the present work is less good. At low frequency, however, good agreement is still obtained, even at large separation.

Finally, in figure 10, we consider a semi-permeable barrier which extends from the bottom partway to the surface (in the example shown, the breakwater has a height equal to $0{\cdot}9h$ where $h$ is the water depth). For this problem, the blockage coefficient $C(y)$ is no longer infinite or zero. We take

$$C(y) = \lambda\left(\frac{1}{(h-y)} - \frac{1}{0{\cdot}9h}\right) \qquad (5.1)$$

so that the blockage coefficient is infinite at $y = -h$ and decreases linearly to zero for $|y| \leqslant 0{\cdot}1h$. It should be noted that $C(y)$ is assumed real here, so that no viscous dissipative effects are included. Such effects can be modelled by allowing $C(y)$ to have a non-zero imaginary part.

An increase in the parameter $\lambda$ corresponds to a decrease in the permeability of the barrier, i.e. the barrier will present a greater obstruction to the flow. This problem, therefore, may be regarded as a first approximation to reflexion of water waves by a rock-fill breakwater. Since thickness effects are not included one would generally expect greater wave reflexion in a real breakwater.

For every small $\lambda$, one would expect only very low wave reflexion. This is borne out by the computer results. As $\lambda$ becomes larger, the transmission would be expected to decrease; this is indeed the situation. For large wave frequency, the transmission coefficient approaches unity. Again, this is to be expected, since very short waves are confined to a thin surface layer and so do not 'feel' the barrier.

The author gratefully acknowledges the help and support given by his supervisor, Professor E. O. Tuck, throughout the course of this work. The research was supported by an Australian Commonwealth Postgraduate Award.

## REFERENCES

ABRAMOWITZ, M. & STEGUN, I. A. 1964 *Handbook of Mathematical Functions.* Washington: National Bureau of Standards.

DEAN, W. R. 1945 On the reflection of surface waves by a submerged plane barrier. *Proc. Camb. Phil. Soc.* **41**, 231–238.

GUINEY, D. C. 1972 Some flows through a hole in a wall in viscous and non-viscous fluids. Ph.D. Thesis, University of Adelaide.

LEWIN, M. 1963 The effect of vertical barriers on progressing waves. *J. Math. & Phys.* **42**, 287–300.

MACASKILL, C. 1977 Ph.D. Thesis, University of Adelaide.

MACASKILL, C. & TUCK, E. O. 1977 Evaluation of the acoustic impedance of a screen. *J. Aust. Math. Soc.* B **20**, 46–61.

MEI, C. C. 1966 Radiation and scattering of transient gravity waves by vertical plates. *Quart. J. Mech. Appl. Math.* **19**, 417–440.

MEI, C. C. & BLACK, J. L. 1969 Scattering of surface waves by rectangular obstacles in waters of finite depth. *J. Fluid Mech.* **38**, 499–511.

MORSE, R. M. & INGARD, K. V. 1968 *Theoretical Acoustics.* McGraw-Hill, New York.

PACKHAM, B. A. & WILLIAMS, W. E. 1972 A note on the transmission of water waves through small apertures. *J. Inst. Maths. Applics.* **10**, 176–184.

PORTER, D. 1972 The transmission of surface waves through a gap in a vertical barrier. *Proc. Camb. Phil. Soc.* **71**, 411–421.

PORTER, D. 1974 The radiation and scattering of surface waves by vertical barriers. *J. Fluid Mech.* **63**, 625–634.

SHERIDAN, D. J. 1975 Computation of the velocity potential for a pulsating source in a fluid with free surface and finite depth. *David W. Taylor Naval Ship Res. and Devel. Center, Rep.* SPD 625-01.

THORNE, R. C. 1953 Multipole expansions in the theory of surface waves. *Proc. Camb. Phil. Soc.* **49**, 707–716.

TUCK, E. O. 1969 Calculation of unsteady flows due to small motions of cylinders in a viscous fluid. *J. Engng Maths.* **3**, 29–44.

TUCK, E. O. 1971 Transmission of water-waves through small apertures. *J. Fluid Mech.* **49**, 65–74.

TUCK, E. O. 1975 Matching problems involving flow through small holes. In *Advances in Applied Mechanics* (ed. C. S. Yih), vol. 15, pp. 89–158. New York: Academic.

URSELL, F. 1947 The effect of a fixed vertical barrier on surface waves in deep water. *Proc. Camb. Phil. Soc.* **43**, 374–382.

WEHAUSEN, J. V. & LAITONE, E. V. 1960 Surface waves. In *Handbuch der Physik* (ed. S. FLUGGE), vol. 9, pp. 446–778.